Prevailing impacts of river management on microplastic transport in contrasting US streams

Kukkola, Anna; Runkel, Robert L.; Schneidewind, Uwe; Murphy, Sheila F.; Kelleher, Liam; Smith, Greg Sambrook; Nel, Holly Astrid; Lynch, Iseult; Krause, Stefan

DOI:
10.1016/j.watres.2023.120112

Document Version
Publisher's PDF, also known as Version of record

Citation for published version (Harvard):
Kukkola, A, Runkel, RL, Schneidewind, U, Murphy, SF, Kelleher, L, Smith, GS, Nel, HA, Lynch, I & Krause, S 2023, 'Prevailing impacts of river management on microplastic transport in contrasting US streams: rethinking global microplastic flux estimations', *Water Research*, vol. 240, 120112.
https://doi.org/10.1016/j.watres.2023.120112

Water Research 240 (2023) 120112

Contents lists available at ScienceDirect

Water Research

journal homepage: www.elsevier.com/locate/watres

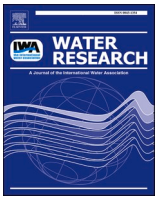

Prevailing impacts of river management on microplastic transport in contrasting US streams: Rethinking global microplastic flux estimations

Anna Kukkola [a,*], Robert L. Runkel [b], Uwe Schneidewind [a], Sheila F. Murphy [c], Liam Kelleher [a], Gregory H. Sambrook Smith [a], Holly Astrid Nel [d], Iseult Lynch [a,e], Stefan Krause [a,e,f]

[a] School of Geography, Earth and Environmental Sciences, University of Birmingham, Edgbaston, Birmingham B15 2TT, United Kingdom
[b] U.S. Geological Survey, Colorado Water Science Center, 3215 Marine St, Boulder, Colorado 80303, United States
[c] U.S. Geological Survey, Water Resources Mission Area, 3215 Marine St., Boulder, Colorado 80303, United States
[d] Centre for Environment, Fisheries and Aquaculture Science, Pakefield Road, Lowestoft, Suffolk NR33 0HT, United Kingdom
[e] Institute of Global Innovation, University of Birmingham B15 2SA, Birmingham. United Kingdom
[f] LEHNA- Laboratoire d'ecologie des hydrosystemes naturels et anthropises, University of Lyon, Darwin C & Forel, 3-6 Rue Raphaël Dubois, Villeurbanne 69622, France

ARTICLE INFO

Keywords:
Microplastics in rivers
Water management
Diversions
Abstraction
Paired catchment approach
Global models

ABSTRACT

While microplastic inputs into rivers are assumed to be correlated with anthropogenic activities and to accumulate towards the sea, the impacts of water management on downstream microplastic transport are largely unexplored. A comparative study of microplastic abundance in Boulder Creek (BC), and its less urbanized tributary South Boulder Creek (SBC), (Colorado USA), characterized the downstream evolution of microplastics in surface water and sediments, evaluating the effects of urbanization and flow diversions on the up-to-downstream profiles of microplastic concentrations and loads. Water and sediment samples were collected from 21 locations along both rivers and microplastic properties determined by fluorescence microscopy and Raman spectroscopy. The degree of catchment urbanization affected microplastic patterns, as evidenced by greater water and sediment concentrations and loads in BC than the less densely populated SBC, which is consistent with the differences in the degree of urbanization between both catchments. Microplastic removal through flow diversions was quantified, showing that water diversions removed over 500 microplastic particles per second from the river, and caused stepwise reductions of downstream loads at diversion points. This redistribution of microplastics back into the catchment should be considered in large scale models quantifying plastic fate and transport to the oceans.

1. Introduction

Microplastics (plastic particles <1 mm) (Hartmann et al., 2019) (here within referred to as MP) are considered to be contaminants of concern (Lambert and Wagner, 2018) and are omnipresent in all environmental compartments on a global scale (e.g.,Bian et al., 2022; Kukkola et al., 2022; Samandra et al., 2022; Zhang et al., 2021). Despite MPs having been the focus of intense research efforts, the sources, their environmental entry points, transport mechanisms and resulting distribution in the environment have yet to be fully understood.

It has been demonstrated that rivers represent major MP transport pathways to the oceans (Lebreton et al., 2017; Meijer et al., 2021), but can also act as long-term sinks (Drummond et al., 2020, 2022; Margenat et al., 2021). Additionally, MPs in riverine environments may undergo major physio-chemical transformation processes (Krause et al., 2021; McGivney et al., 2020) and interact with the diverse community of freshwater organisms with potentially detrimental effects on species and ecosystem health (e.g., causing entanglement, suffocation, and intestinal damage) (Anbumani and Kakkar, 2018; Kukkola et al., 2021).

To fully assess the risks that MPs pose to river environments and their ecosystem services, it is important to understand how MPs are distributed within river corridors and how they get transported and potentially accumulated in river networks (Krause et al., 2021). Previous research has highlighted the existence of substantial spatial variability in MPs in surface water and sediment in a wide range of river systems (e.g., Castañeda et al., 2014; Kurki-Fox et al., 2023; Wong et al., 2020). However, it is less well-established which processes control this spatial variability. A better understanding of these processes may result in more accurate

* Corresponding author.
E-mail addresses: ATK863@bham.ac.uk, Anna.Kukkola@outlook.com (A. Kukkola).

https://doi.org/10.1016/j.watres.2023.120112
Received 12 December 2022; Received in revised form 11 May 2023; Accepted 20 May 2023
Available online 24 May 2023

predictions of the full extent to which rivers contribute to global plastic fluxes into the oceans and for site-specific risk assessments. Additionally, flux information may be coupled with estimates of MP residence times, to assess local exposure and potential impacts on freshwater ecosystems. This could lead to a better understanding of the potential sources and guide any regional management and mitigation strategies.

Previous research has aimed to identify how population density and specifically, the location of potential point and diffuse sources of discarded plastic waste influence the spatial distribution of MP. Consequently, land use/land cover has been linked to MP concentration and distribution in rivers (Grbić et al., 2020; Wang et al., 2021), and global scale estimates of terrestrial plastic pollution and resulting riverine contributions to the oceans have predicted pollution hotspots to occur in densely populated urban areas with poor waste management systems (Ferraz et al., 2020; Lebreton et al., 2019, 2017; Meijer et al., 2021). However, a clear correlation between the degree of urbanization and MP concentration could often not be established (See Talbot and Chang, 2022 for a review; Tibbetts et al., 2018).

There is growing awareness that, in addition to the spatial distribution of sources, the environmental fate of MPs is strongly determined by their transport, dispersal and potential deposition and storage along river networks (de Carvalho et al., 2021; Margenat et al., 2021; Tibbetts et al., 2018). Flow conditions may strongly affect MP deposition behaviour and residence time in the hyporheic zone (Drummond et al., 2020, 2022). Current model predictions of riverine contributions to MP in the world's oceans show discrepancies ranging over several orders of magnitude (Lebreton et al., 2017; Schmidt et al., 2017). Current models use only relatively coarse spatial information of river discharge, if included at all (Siegfried et al., 2017; Uzun et al., 2022; van Wijnen et al., 2019). Very few studies have investigated the change in MP concentrations in relation to the hydrological regime and the characteristic flow and transport behaviour of the respective river systems (Campanale et al., 2020; Wagner et al., 2019). A general assumption of existing large scale plastic transport models is a downstream convergence of particle fluxes along the river network. There is a severe lack of understanding of the impact of river water management schemes (e.g., water diversion for irrigation and drinking water), on MP distribution, fate, and transport in river corridors, despite the majority of rivers globally now being regulated in their flow (Barbarossa et al., 2020; Baumgartner et al., 2022). It may therefore be important to analyse and quantify the combined impacts of MP source distributions, and their transport in river networks under the influence of anthropogenically altered flow and transport conditions, in order to aid model predictions.

Here, we present a comparative field study that applies a paired-catchment approach to quantify the spatial distribution of MP in two neighbouring catchments (South Boulder Creek and Boulder Creek, Colorado, USA) with different degrees of urbanization. This study aims to (i) characterize the downstream evolution of MP concentration and associated particle properties in surface water and streambed sediments, (ii) identify MP source areas using spatial profiles of stream load (the product of concentration and stream discharge), (iii) evaluate the effects of a) the mountain to plains transition and b) urbanization, and (iv) quantify the degree to which flow diversions affect MP concentrations, loads, and downstream transport.

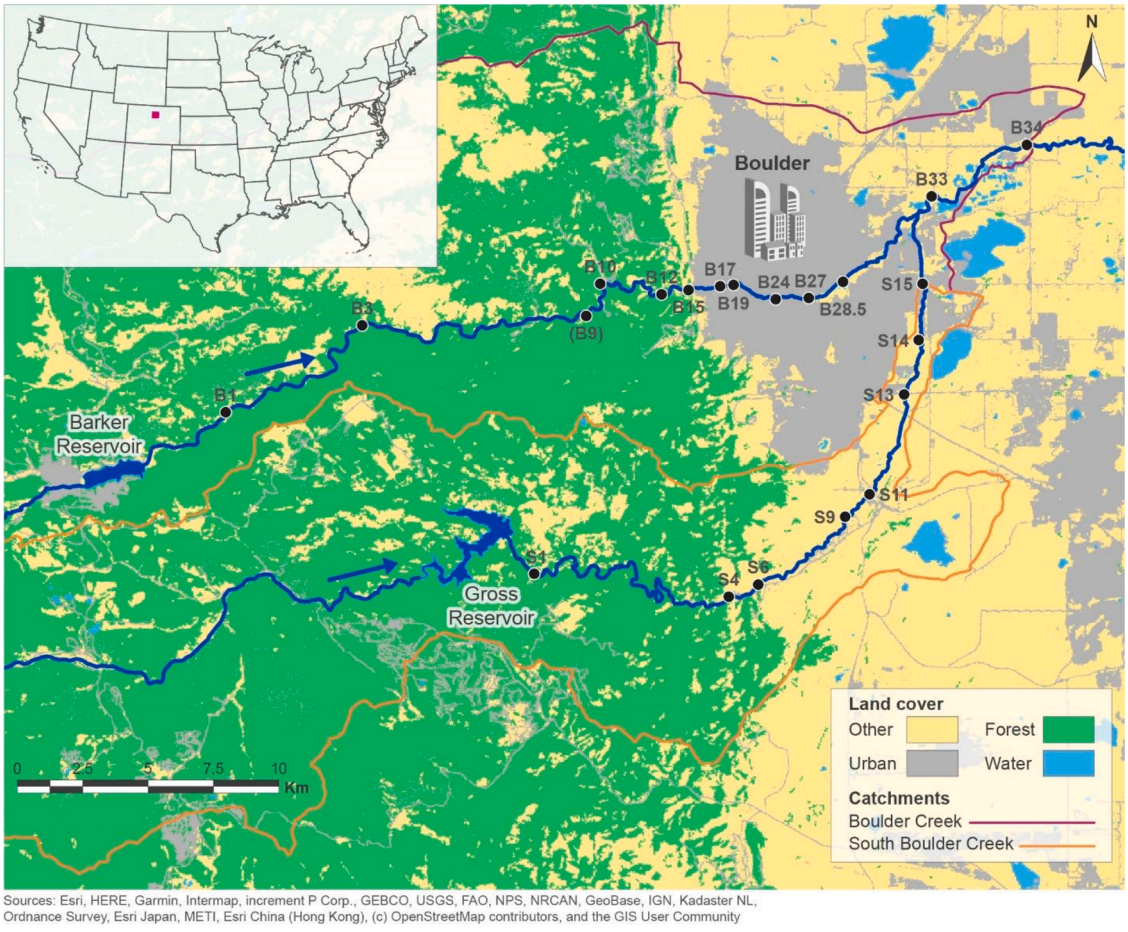

Fig. 1. Map of catchment areas indicating major land cover classes (Section 2.4) and sampling locations (black dots) along Boulder Creek (B1–34) and South Boulder Creek (S1–15), Colorado, USA. Blue arrows indicate flow direction and orange and pink lines the extent of SBC and BC catchment areas, respectively. Coordinates of each sampling location are provided in Table S1. Land cover class "Other" includes perennial ice/snow, barren land, grassland, shrub/scrub, cultivated crops, and pastry-hay.

2. Materials and methods

2.1. Study region

Boulder Creek (BC) and its tributary South Boulder Creek (SBC) (Colorado, USA) are part of the wider Boulder Creek Watershed, which extends over 1160 km^2 and is located in the Front Range of the Rocky Mountains, east of the Continental Divide. Both catchments cover diverse geographical and hydro-geomorphological conditions along a rural-urban gradient and differ significantly in catchment-wide and near-stream land cover patterns (Fig. 1).

Both streams flow northeast from their mountainous headwaters that originate at the Continental Divide (elevations >4100 m) and through canyons (upstream sampling locations B1 and S1 are ~2400 m; sampling locations are further described in Runkel et al., 2022) before they reach the plains (sampling locations B12 and S6, elevation <1800 m), and eventually confluence at the eastern edge of the city of Boulder near sampling point B33 (Fig. 1). Ultimately these waters drain into the Mississippi River and the Gulf of Mexico, over 2300 km away. The BC catchment is more urbanized (12% upstream of confluence with SBC) than SBC (3.9% upstream of confluence with BC). Both are characterized by a high forest cover (BC 73% and SBC 84%). The catchment areas for BC and SBC upstream of their confluence are 405 km^2 and 342 km^2 respectively, with a total catchment size of 790 km^2 at point B34 (Fig. 1). The sampled river sections cover 36.7 km flow length of BC and 27.7 km of SBC. Over these sections, river slope varies between 0.003 m/m (B34) and 0.040 m/m (B9) for BC and 0.005 m/m (S9) and 0.085 (S1) for SBC while average sinuosity is 1.31 (BC) and 1.39 (SBC), respectively, indicating a comparable, and generally low degree of meandering. (The procedures used to determine the foregoing watershed characteristics are detailed in Section 2.4).

Like for many river systems in the western United States, water management plays a large role in both streams (Murphy, 2006). Mountain reservoirs are used to store large volumes of water generated during spring snowmelt, and this water is subsequently diverted out of the catchments for municipal and agricultural use through a system of canals. As such, stream discharge decreases in downstream direction for long periods of the year.

The BC study reach begins approximately 4 km downstream of Barker Reservoir, which receives water from the surrounding catchment, a relatively undeveloped area to the east of the Continental Divide. Water released from Barker Reservoir travels down Boulder Canyon, entering the City of Boulder near sampling location B12 (Fig. 1). The primary diversion affecting stream discharge during this study is located downstream of sample location B19, where more than half of the discharge is diverted away from BC at certain times of year (Murphy, 2006).

The SBC study reach begins approximately 1.5 km downstream of Gross Reservoir which receives much of its water from the underground Moffatt Tunnel that transports water from west of the Continental Divide to the eastern side (Murphy, 2006). Most of the water leaving Gross Reservoir is diverted out of SBC downstream of sampling location S1, supplying water to the city of Denver. SBC flows through the small town of Eldorado Springs (between S4 and S6, Fig. 1) before entering the plains downstream of sample location S6. A second major diversion active during the study period is located downstream of site S13, resulting in additional decreases in stream discharge.

2.2. Field data and sample collection

Surface water and sediment samples were collected from thirteen locations within BC and eight sites within SBC (as a subset of a larger study that included additional sample locations; Runkel et al., 2022). Sampling took place October 14–18, 2019, during steady low-flow conditions, which are typical in the research area for the period between October and March. The relatively steady flow conditions during the sampling period were confirmed by stream discharge records from gauging stations BOCOROCO (~18.5 km downstream from Barker Reservoir, sampling location B9) and BOCELSCO (~0.7 km downstream from the major diversion located between S1 and S4) (https://www.dwr.state.co.us, Fig. 2).

At each sampling site, 50 L of surface water was collected from the centre of the stream, and from the middle depth (due to low flow conditions ~10 cm) of the water column with galvanized metal bucket. During sampling the bucket was lowered into the stream horizontally, opening facing upstream. The bucket was returned to the upright position after being filled by the flowing water and the surface water was filtered through a 63 μm nylon mesh, from which contents were then transferred into a precleaned 20 mL glass vial using deionized water. The MP samples collected in this manner are assumed to include buoyant MPs and MPs with a density greater than water that have yet to settle to the streambed. Suspended sediment sampling techniques (Edwards and Glysson, 1999) were not employed in this study given the steady low-flow conditions in which bedload is assumed to be negligible contributor to constituent load.

Sediment was collected from both streambanks just above the water line using a metal spoon. A composite sediment sample from three spots (within a radius of about 1 m) was collected and stored in a clean glass jar, giving a final sample mass of 60 - 90 g per streambank. All samples ($N_{water} = 21$ and $N_{sediment} = 42$) were stored at room temperature and transported to the University of Birmingham, UK for analysis at the end of the sampling period. Data collected at each sampling point comprised geographic coordinates, stream depth, cross-sectional area, velocity, and discharge as measured by Acoustic Doppler Velocimetry (Table S1; Runkel et al., 2022).

2.3. Sample analysis and QA/QC

Sediment and water samples were extracted using sediment-MP isolation (SMI) units in accordance with Nel et al. (2020), as described in supplementary section S1 MP extraction. After extraction, organic matter (OM) was digested using Fenton reagent and stained with Nile Red as described in section S1. Samples were analysed with fluorescence microscopy as described in Kukkola et al., 2023 and section S2. Polymer identification by confocal Raman spectroscopy (Lenz et al., 2015; Kelleher et al., 2023) was employed for roughly 44% of all putative MPs (in total 206 particles). The procedure and spectra acquisition parameters are described in section S3. Field background samples, laboratory blanks and positive blanks were collected and analysed as described in S4. For the purposes of this study, MP measurements in counts per litre are hereinafter referred to as concentrations.

2.4. Land cover, population density, and statistical analyses

To understand how MP concentrations vary in relation to catchment area and the percent of urban land cover, each sub-catchment (defined as the drainage area discharging towards each sampling location) was delineated with the USGS program StreamStats v4.6.2 (U.S. Geological Survey, 2019) and exported into ArcMap 10.7.1 (ESRI, 2011). Population density per sub-catchment for 2019 was obtained from the Colorado State Demography Office (https://demography.dola.colorado.gov) and land cover classes for sub-catchments were determined utilizing the National Land Cover Database (NLCD) (Multi-Resolution Land Characteristics Consortium; https://www.mrlc.gov/viewer/) 2019 dataset which contains official land cover data for the USA (2019) with a resolution of 30 × 30 m. The 20 landcover classes from the NLCD data set were reclassified into nine general categories (see supplementary section S5).

To analyse potential local land cover impacts on observed MP concentrations, a 500 m circular buffer ($A = 0.79$ km^2) was created around each sampling site in ArcMap, to aid identification of possible local source effects, as compared to the sub-catchment wide approach. To

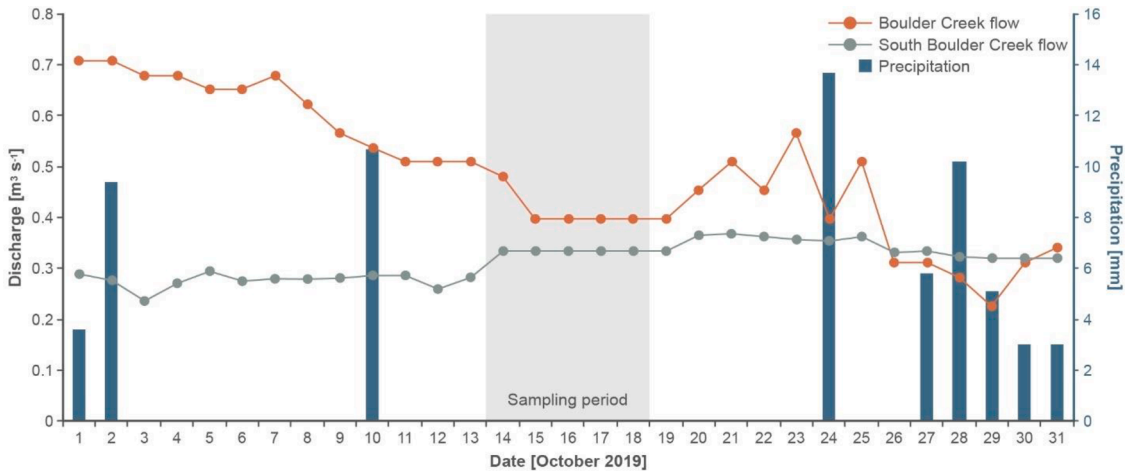

Fig. 2. Discharge and precipitation during the sampling period in October 2019. Discharge data are from the Colorado Division of Water Resources gauges BOCOROCO near Orodell, CO (B9 Fig. 1) and BOCELSCO near Eldorado Springs, CO (https://www.dwr.state.co.us). Precipitation data are from the National Oceanic and Atmospheric Administration Physical Sciences Laboratory, located at 39.99271N, −105.2652W (Wetherbee et al., 2021).

study effects in sub-catchments, the area per land cover class was normalized to the respective sub-catchment area. Data were assessed for normality using a Shapiro-Wilk Test. Spearman's rank coefficient was used to determine correlations between MP concentrations and urban land cover and population density, because MPs data followed a non-normal distribution.

To evaluate any variation in MPs concentrations in water and sediment between and within the two streams, Mann-Whitney U and Kruskal-Wallis tests were applied. Spearman's rank coefficient was used to assess correlation direction and strength for MP concentration and size (measured as longest length) and hydrological parameters. All statistical analyses were carried out in RStudio (R Core Team 2022) with a significant threshold of $\alpha = 0.05$.

2.5. MP loads and estimated concentrations in the absence of diversions

Contributions of MPs from the sub-catchments discharging to each segment of the study reaches (i.e., the distance between sampling locations) were quantified using spatial profiles of the stream MP loads (Table 1), developed by summing the observed load at each location (the product of stream discharge and concentration) and the load that had been diverted out of the system (the product of the diverted stream discharge and the concentration at the nearest upstream site). Profiles of cumulative load were calculated by summing all positive changes in instream load, while keeping the cumulative load constant when the instream load decreased (Kimball et al., 2002; Runkel et al., 2013). Stream segments with increases in cumulative load thus represent source areas, with each source area contributing a percentage to the overall load:

$$percent\ contribution = 100 \times \frac{(L_d - L_u)}{(L_b - L_t)} \quad (1)$$

where $\boldsymbol{L}$ is the cumulative load, $\boldsymbol{d}$ and $\boldsymbol{u}$ denote the cumulative load at the downstream and upstream ends of a stream segment, while $\boldsymbol{b}$ and $\boldsymbol{t}$ denote the cumulative load at the bottom and top of the study reach.

Loading rates (change in load per km) were also calculated for individual segments (between sampling points) and for the entire study reach as:

$$Loading\ rate = \frac{\Delta\ load}{distance} \quad (2)$$

where $\boldsymbol{\Delta\ load}$ is the change in load for the segment or study reach ($\boldsymbol{L_d} - \boldsymbol{L_u}$ or $\boldsymbol{L_b} - \boldsymbol{L_t}$) and distance equals the length of the segment or study reach (Table 1). Three sampling points were excluded from the loading

Table 1
Microplastic (MP) total, diverted and cumulative loading rates for Boulder Creek (site IDs B1-B28.5) and South Boulder Creek (site IDs S1-S15).

Site ID	Distance from reservoir [m]	Stream Discharge [L s^{-1}]	Total Diverted stream flow [L s^{-1}]	Surface water MP concentration [MP L^{-1}]	Observed (Obs) load [MP s^{1}]	Total Diverted (Div.) load [MP s^{-1}]	Obs + Div [MP s^{-1}]	Cumulative Obs + Div. load [MP s^{-1}]	Percent Contribution [%]	Loading rate [MP s^{-1} km^{-1}]	No Div. Conc [MP L^{-1}]
B1	3719	292	0	0.12	35	0	35	35			0.12
B3	9711	230	0	0.12	28	0	28	35			0.12
B9	18,150	399	0	0.04	16	0	16	35			0.04
B10	19,676	453	0	0.17	77	0	77	96	34%	40	0.17
B12	22,266	500	0	0.26	130	0	130	149	30%	20	0.26
B24	26,073	119	426	0.62	74	119	193	212	36%	17	0.35
B27	27,097	140	426	0.26	36	119	156	212			0.28
B28.5	28,272	138	426	0.16	22	119	141	212			0.25
S1	1515	2485	0	0.16	398	0	398	398			0.16
S4	12,319	179	2418	0.02	4	377	381	398			0.15
S6	13,354	248	2350	0.06	15	376	391	407	25%	10	0.15
S9	17,352	293	2350	0.04	12	376	388	407			0.15
S11	18,454	288	2361	0.08	23	376	400	419	29%	11	0.15
S13	21,952	300	2361	0.12	36	376	413	432	32%	4	0.16
S14	23,848	63	2598	0.14	9	405	414	433	3%	1	0.16
S15	25,630	81	2598	0.16	13	405	418	438	11%	2	0.16

analysis due to unsteady flow conditions during sampling (B15, B17 and B19). Two additional BC sites (B33, B34) were also excluded as they are located below the confluence of BC and SBC and are not used in the comparison of the two study reaches. These downstream sites are omitted from our discussion of the results presented in Sections 3.1 and 3.3

Both study reaches have water diversions which decrease stream discharge. Sampling locations downstream of these diversions will have a smaller volume of water than they would in the absence of diversions, and consequently the impact of a given source area and loading rate will be exacerbated with less dilution occurring due to reduced discharge. These impacts can be formally quantified by estimating the MP concentrations that would be observed in the absence of diversions. MP water concentrations in the absence of diversions are calculated by summing the observed and diverted loads and dividing by the sum of the observed and diverted stream discharge.

3. Results

3.1. Stream discharge

Several flow diversions were active during the sampling event, and 85% of the stream discharge present at B12 was diverted away from BC between B12 and B24 (0.43 $m^3 s^{-1}$, Fig. 3a) and from 0.06 $m^3 s^{-1}$ (S14) to 2.48 $m^3 s^{-1}$ (S1) for SBC (Fig. 3b). Several flow diversions were active during the sampling event, with the major diversion on BC diverting 87% of the stream discharge at B19 away from BC (0.43 $m^3 s^{-1}$). For the SBC study reach, 95% of the stream discharge at S1 (2.35 $m^3 s^{-1}$) was diverted for use by the city of Denver and 79% of the remaining stream discharge at S13 (0.24 $m^3 s^{-1}$) was diverted out of the channel.

3.2. MP concentrations in surface water and streambed sediments

MP were detected in all surface water and sediment samples across the studied sites (Fig. 4). Mean surface water concentrations for BC were 0.22 MP L^{-1} (± 0.14 standard deviation (SD)), ranging between 0.08 (B9) and 0.62 MP L^{-1} (B24). For SBC, mean MP concentrations were 0.09 MP L^{-1} (± 0.05 SD) with a range between 0.02 (S4) and 0.16 MP L^{-1} (S1). A Mann-Whitney U test confirmed that the difference in MP concentration in the surface water between the two streams was significant ($p = 0.016$). Streambed sediments for BC had a mean dry-weight concentration of 186 MP kg^{-1} (± 80 SD), ranging between 114 (B3) and 342 MP kg^{-1} (B24). For SBC the mean sediment concentration was 142 MP kg^{-1} (± 55 SD), ranging from 98 (S1) to 214 MP kg^{-1} (S11). Mann-

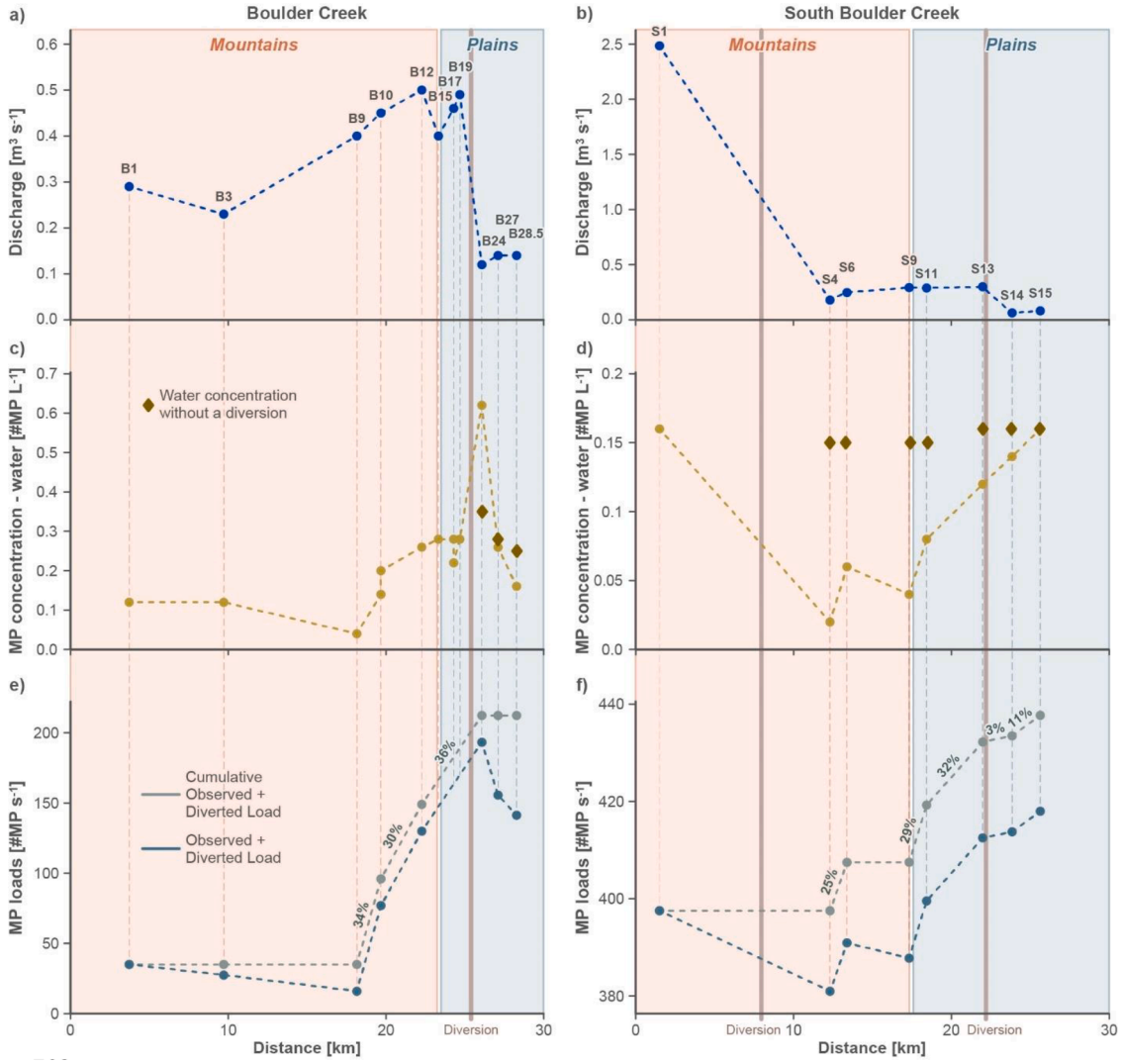

Fig. 3. Stream discharge (panels a-b; Runkel et al., 2022), MP surface water concentrations [#MP L^{-1}] and estimated concentrations in the absence of diversions (panels c-d), and downstream profiles of MP loads [#MP s^{-1}] (panels e-f) for Boulder Creek and South Boulder Creek. Note replicate samples collected at B10 and B17 (panel c). Information presented in panels c-f is presented in Table S1 and/or available from the first author.

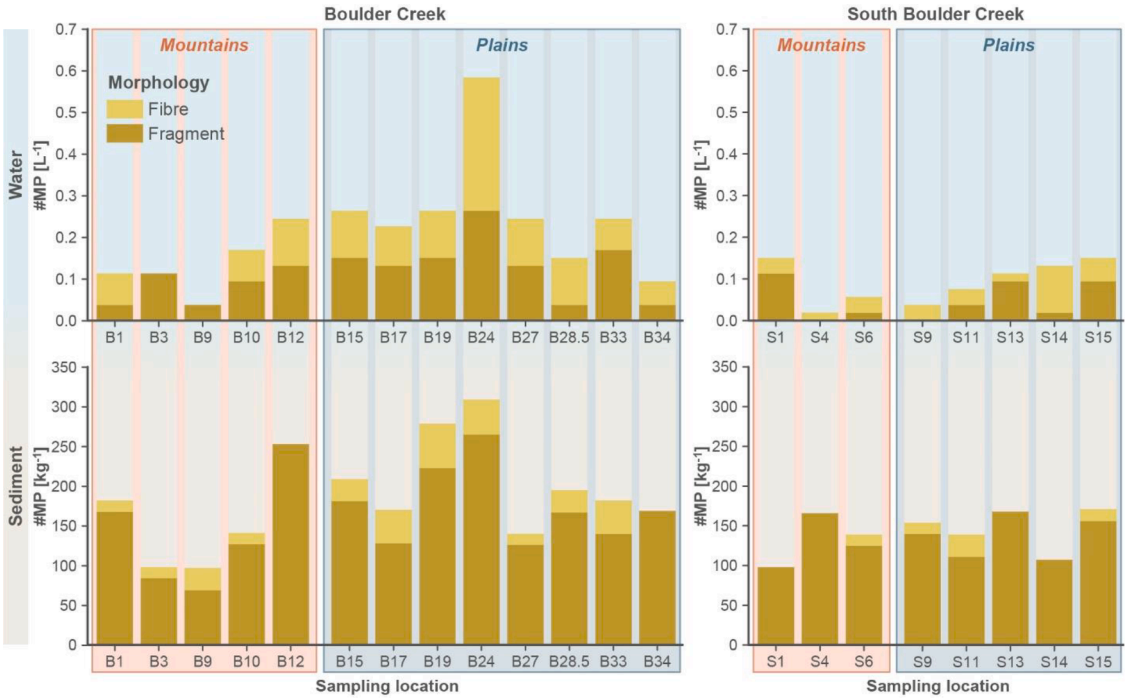

Fig. 4. MP concentration distribution in water (top panel) and sediments (bottom panel) of Boulder Creek (left) and South Boulder Creek (right) (Table S1).

Whitney Test indicated that the difference in sediment concentration was non-significant ($p = 0.091$).

The sediment concentrations generally displayed a non-significant increasing trend downstream, with peaks between sites B12 and B24 (Fig. 4), B12 being where BC emerges from Boulder Canyon at the city margins of Boulder, while B24 is located at the eastern edge of a high-density urban area where the highest surface water concentration was also observed.

Peak water MP concentrations at SBC were recorded at the most upstream site (S1) and the most downstream site (S15) (0.16 MP L^{-1}); the highest MP concentrations in SBC sediment were recorded at site S11. Surface water concentrations in SBC exhibited a linear positive relationship with distance downstream of the first major diversion (site S1 excluded; R_s=0.964, $p = 1.85 \times 10^{-5}$), with increasing concentrations downstream. A similar, but non-significant, trend was also observed in sediments (Fig. 4).

No correlation was found between stream discharge and the size of MP either in surface water or sediments at BC; however, a moderate positive correlation was found between discharge and size of MPs in surface water at SBC (Table S4). There was no correlation between discharge and MP concentration in water or sediments (Table S5). No correlation was found between river velocity or slope and MP concentration in surface water or sediments (Table S5).

3.3. MP loads

The average stream MP load for BC was 97 MP s^{-1}, with a range between 16 MP s^{-1} (B9) and 193 MP s^{-1} (B24) (Fig. 3e). The stream MP load for BC declines from B1 (35 MP s^{-1}) to B9 (16 MP s^{-1}), after which it steadily increases to its maximum of 193 MP s^{-1} at B24. MP load then decreases in the last two stream segments (B27 and B28.5), to 141 MP s^{-1} (Fig. 3e).

The average stream load for SBC was 400 MP s^{-1}, with a range between 381 MP s^{-1} (S4) and 418 MP s^{-1} (S15) (Fig. 3f). The MP stream load drops between sites S1 and S4, after which it generally increases to its maximum value at the end of the study reach (S15, Fig. 3f). As will be discussed in detail in Section 4.4, most of the stream load is diverted out of the SBC catchment near the head of the study reach.

Average study-reach loading rates were 7.2 and 1.7 MP s^{-1} km^{-1} for BC and SBC, respectively. MP loading in BC is dominated by contributions to the three stream segments ending at B10, B12, and B24 (percent contributions of 34, 30, and 36% respectively; Fig. 3e). MP loading at SBC had major contributions at S6 (25%), S11 (29%), S13 (32%), and S15 (11%) (Fig. 3f).

3.4. Physical and chemical properties of MP

For BC surface water, fragments amounted to 51.7% and fibres to 48.3% of the total MP detected (Fig. 4). Similarly, for SBC surface water, 51.3% of total MP were fragments and 48.7% fibres. No spheres were detected in water samples from either stream. A clear colour dominated fragments and a blue colour dominated fibres in both streams. In the BC sediments, mostly fragments were present (87%), while fibres (12%) and spheres (1%) played a minor role (Fig. 4). For SBC the percentage of fragments (93%) was slightly larger while fibres only amounted to 7%. In sediments from both streams, most fragments were a clear colour while most fibres were black. In total, 206 putative MPs (44% of total) were subjected to Raman spectroscopy analysis from which 86% were positively identified as plastics, with the most common polymer type in surface water being polyester (50%) and in sediment being polyethylene terephthalate (36%, for details see supplementary section S6). The respective identification rate for fragments was 75% and 92% for fibres.

3.5. Land cover impacts on mp

A Mann Whitney U test indicated a statistically significant difference in urban land cover between BC and SBC upstream of their confluence ($U = 84$, $p = 0.0001$). When assessing the relationship of urban land cover within sub-catchments to MP concentrations, no correlation was found in water or sediments for BC. However, at SBC, a very strong correlation was found in surface water (site S1 excluded; R_s=0.964, $p = 1.85 \times 10^{-5}$), with no trend evident in the sediments (SBC Rs -0.047, $p = 0.910$). Besides urbanization, no significant correlations were found for other land cover types for SBC. MP concentrations in surface water were positively correlated with forest cover (Rs=0.643, $p = 0.024$) for BC, but negatively for SBC (Rs =-0.658, $p = 0.075$). This is likely due to forest

cover in BC increasing downstream towards the confluence but decreasing downstream at SBC towards more urbanized areas, suggesting that. MP concentrations in surface water and sediment were not correlated with the total catchment area (BC_{water} Rs=0.275 $p = 0.391$, BC_{sed} Rs=0.322 $p = 0.222$, SBC_{water} Rs=0.395 $p = 0.332$ SBC_{sed} Rs=0.476 $p = 0.232$).

The analysis of land cover impacts in the immediate 500 m buffer around each sampling location revealed a strong positive correlation between surface water MP concentration and urban cover at BC (Rs=793, $p = 0.025$), and at SBC if the most upstream sampling point (S1) was excluded from the analysis ($Rs_{withS1=.0}299$, $p = 0.4713$, $Rs_{withoutS1}$=0.828, $p = 0.023$). For sediments, no significant correlation was identified for BC (Rs=0.508, $p = 0.075$) while for SBC the moderate correlation found was not statistically significant (Rs=0.547, $p = 0.160$). None of the other land cover types had any correlation to MP concentrations for BC or SBC.

4. Discussion

4.1. MP concentration in surface water and sediments

The more urbanized BC (0.22 MP L^{-1}, >63 μm) had higher MP concentrations in surface water than SBC (0.09 MP L^{-1}), but both streams could be considered to have relatively low MP contamination present and our findings are similar to other studies in rivers of comparable properties (remote, mountainous) (Bian et al., 2022; Dalmau-Soler et al., 2021; Ferraz et al., 2020) and orders of magnitude lower than those reported from lowland rivers, such as canals in Suzhou city, China (8 - 40 MP L^{-1}) (>20 μm) or Amsterdam, Netherlands (48 -187 MP L^{-1}) (>10 μm) (Jin et al., 2022; Leslie et al., 2017). Similarly, BC had higher sediment MP concentrations (186 MP kg^{-1}) than SBC (142 MP kg^{-1}), but these are in line with those previously reported from remote areas, such as from the rivers of the Tibetan Plateau, (50 - 195 MP kg^{-1} >20 μm) (Jiang et al., 2019) and from Dafeng River, China, (0.0 - 50.3 MP kg^{-1} >20 μm).

4.2. The effects of the mountain to plains transition and urbanization on MP concentrations and types

Surface water and sediment MP concentrations increase in the downstream direction for both BC and SBC, with downstream trends being particularly clear in surface water (Fig. 4). This is consistent with previous studies: six rivers located at a mountain-foothill transition area in the Chin Ling - Wei River Plain, China, had concentrations of 2.57 ± 0.14 MP L^{-1} (>75 μm) in the mountainous areas, with increasing concentrations of MP downstream (up to 20.40 ± 0.43 MP L^{-1}), which coincided with an increase of polyethylene films downstream (Bian et al., 2022). Similarly, in the Llobregat River, Spain, no MPs (>20 μm) were reported from headwater locations, but concentrations increased downstream to 3.60 MP L^{-1} (Dalmau-Soler et al., 2021). Polyester fibre and fragment concentrations also increased downstream, which was attributed to washing synthetic clothes and non-treated discharge (Dalmau-Soler et al., 2021). This type of downstream change has previously been attributed to increasing population, urbanization, and anthropogenic activity, typically present along the flow length(s) of rivers (de Carvalho et al., 2021; Yuan et al., 2022). These trends therefore suggest a linkage between MP concentration and urbanization, given the increase in urbanization with distance downstream that has been documented in both our catchments. This linkage is further illuminated by the sub-catchment analysis. A positive relationship was detected for MP concentration and degree of urbanization in sub-catchments of SBC downstream of S1. Though this relationship was not found for the sub-catchments of BC, the effect of urbanization was evident in both surface water and sediments, with a clear increase of MP concentrations at B10 where the stream emerges from Boulder Canyon and enters the urban area (Fig. 4). This increase is maintained downstream of B10, with relatively consistent MP concentrations through the highly urbanized area (B10-B27). The effect of urbanization was further supported by assessment of the immediate 0.79 km^2 buffer around sampling points, as this revealed a significant local impact of urbanization in surface water for both BC and SBC (S1 was excluded as an outlier), indicating that proximity to the source and human activities is likely to be a critical factor in driving MP concentration in this riverine environment.

Although data from both streams suggests a linkage between MP concentration and urbanization, the effect of urbanization can be further elucidated by directly comparing the two streams. Urban land cover in the BC catchment is approximately 3.1 times greater than that of SBC (Section 2.1), and the higher degree of urbanization in BC may be responsible for the higher surface water and sediment MP concentrations (Section 3.2). Further, the MP loading rate for the BC study reach is 4.2 times higher than for SBC (Section 3.3), in close agreement with the urban land cover ratio (3.1) and the ratio of loading rates for urban-derived inorganic constituents considered in the larger study that coincided with this research (Runkel et al., 2022).

Sub-catchment contributions of MPs to the receiving streams are formally quantified by the loading analysis. For the case of BC, three consecutive stream segments represent the dominant MP sources, with each contributing approximately one third of the MP load (B10-B24; Fig. 3e, Section 3.3). The sub-reach encompassing these segments begins upstream of the City of Boulder, suggesting the presence of a margin around the urban area that is affected by the more populated area: i.e., access to numerous mountain homes and recreational activities is provided by a heavily travelled highway in the lower part of Boulder Canyon. The lower parts of this sub-reach are within the city proper, and water and sediment concentrations at its terminus are the highest concentrations observed in this study (B24, Section 3.2).

At SBC, higher sub-catchment contributions include S1 at the head of the study reach and stream segments downstream of Eldorado Springs. Although the surface water concentration at S1 is high relative to other SBC sites, S1 is not in an urban area and its concentration is lower than at the urban sites in BC (Fig. 4). The high MP concentration observed at S1 is likely attributable to its proximity to Gross Reservoir, where potential sources include recreational activities, water diverted from west of the Continental Divide, and a nearby road. Though atmospheric deposition has been reported previously for this study area and adjacent Upper Colorado area (Reynolds et al., 2022; Wetherbee et al., 2019), the contribution to MP concentration is expected to remain equal at all sites, and is not believed to be the driving cause of the relatively high MP concentrations at S1. All stream segments downstream of Eldorado Springs contribute to the MP load, except for the segment ending at S9 (Fig. 3f). This loading may also be associated with urban activities, with potential sources being areas such as Eldorado Springs, low-density housing upstream of S11, and highways and roads that cross SBC as it enters the plains.

4.3. The effect of diversions on MP concentrations, loads, and downstream transport

The magnitude of flow diversions from BC and SBC results in large quantities of MP being removed from each catchment, despite the relatively low surface water concentrations observed in both streams. The diversion downstream of B12 removes ~85% of the water (Section 3.1) and an equivalent percentage of surface water MP from BC (a removal of 119 MP s^{-1}: Fig. 5). Similarly, the diversion below S1 removes ~95% of the water and MP (a removal of 376 MP s^{-1}) from SBC, while the second diversion removes ~80% of the remaining water and MPs (removing 29 MP s^{-1}, Fig. 5). While many studies thus far have considered rivers as dendritic conveyor belts where plastics particle fluxes are converging along the transport from land to ocean with certain MP retention times (Hurley et al., 2018; Ockelford et al., 2020), this study's quantitative load analysis suggests that water management may have a

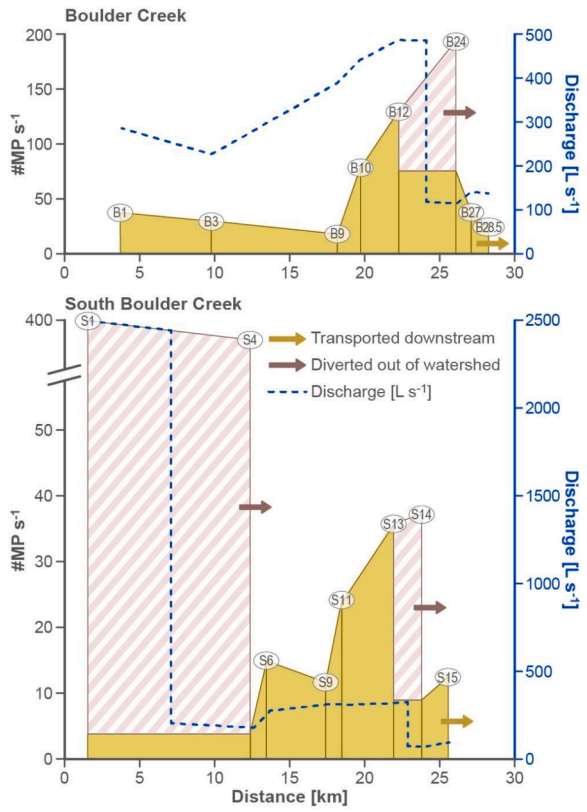

Fig. 5. MP Load (Yellow line), Diverted load (Dashed line) and Discharge (L s^{-1}) shown for a) Boulder Creek and b) South Boulder Creek.

significant impact on MP fate, and the MP flux delivered to the ocean. The eventual fate of diverted MP depends on the diverted water's use. Water used as a source of municipal drinking water may result in the sequestration of MP, given the effectiveness of water treatment plants that remove 80–93% of MPs (>20 μm) from potable water supplies (Dalmau-Soler et al., 2021; Shen et al., 2020). In contrast, water diverted for agricultural purposes re-routs and disperses MPs to the wider terrestrial environment, and these particles may be flushed back into streams in the long term.

Diversions may also have a large impact on MP concentration, fate, and transport in the downstream portions of these managed systems. Estimated MP water concentrations are calculated for sampling locations downstream of large diversions (Section 2.5) and are shown in Fig. 3c-d and Table 1. An example of this effect is B24, the site with the highest MP concentration recorded in this study. B24 is the first sampling location downstream of the large diversion on BC, and its concentration is roughly double that of all other BC locations, despite having a percent contribution to the total load that is comparable to the stream segments above the diversion and a loading rate that is lower (Table 1). This disconnect is explained by the large magnitude of the diversion; the estimated concentration at B24 in the absence of the diversion is similar to that of nearby sites and what appears to be an outlier is just an artefact of the flow regime. A second example of this effect is the large diversion on SBC below S1. With the diversion in place, most of the MP mass is diverted out of the system and what remains in the stream is more easily diluted by waters in the undeveloped portions of the SBC canyon. In the absence of this diversion, MP concentrations at the downstream locations would have the concentration signature of S1, as this large volume of water (and large amount of MP mass) would be relatively unaffected by the sources downstream (Fig. 3d).

Diversions also alter the hydrodynamic conditions of the downstream reach, potentially changing the fate of the MP travelling in the water column. In the case considered here, the diversion on BC causes a dramatic decrease in stream velocity, with a median velocity below the diversion (0.14 m s^{-1}, B24-B28.5) that is roughly half the velocity above the diversion (0.26 m s^{-1}, B1-B19; Table S1). This decrease in velocity increases MP residence time in the stream segment, potentially resulting in increased settling of MP mass to the streambed. In addition, median stream depth decreases below the diversion (0.2 m, B24-B28.5; median 0.3 m, B1-B19), increasing the probability that MP will settle and become entrained in the streambed. The effects of these changes are evident in the loading analysis, with instream loads decreasing in two of the three segments below the diversion (B27 and B28.5, Fig. 3e). This additional loss of MP mass may be attributable to increased settling and retention in the streambed.

In summary, little focus has been given previously to how water management activities affect MP transport downstream, and the effects have not been incorporated into global models to date. The total diverted load within this system was as high as 524 MP s^{-1}, which is a significant finding given that the present study was conducted in a relatively remote mountain watershed over a short spatial scale. It has been estimated that in the year 2012, 241 km^3 of water was diverted for the purpose of agriculture in North America alone, and 2670 km^3 globally (Frenken, 2012). Using values from this study, an estimated 41.39 × 10^{12} MP particles >63 μm are redistributed to the terrestrial environment in North America and as many as 45.93 × 10^{14} (or 459 trillion) MP globally. However, as the numbers for diverted MP used here are only representative of this relatively remote system, this is likely a gross underestimation of the global total, as higher MP concentrations have been reported in lower order streams (up to 25.5 ± 3.5 MP L^{-1} in the Maozhou River) (Kumar et al., 2021; Wu et al., 2020). This implies that diversions located in more polluted systems will unavoidably carry and re-distribute more MP than estimated here, none of which has been integrated into global or regional MP models. In 2020, ~693 million m^3 per capita of surface water was diverted globally for purposes of irrigation, industrial processes, and potable water (OECD, 2022), and extended monitoring of MP in water diversions may help bridge the gap between research and regulations (Coffin, 2023). Further, the water diversions and the MP they divert, have not been accounted for in any of the current global models. The models may therefore overestimate the total amount of MPs flowing into oceans and simultaneously underestimate the quantity ending up in terrestrial ecosystems due to this re-distribution.

4.4. *Advantages of the load approach*

The application of a loading analysis developed for metal contamination (Kimball et al., 2002; Runkel et al., 2013) to an assessment of MP results in several advances in understanding the concentration and fate of this contaminant in streams and rivers. First, stream discharge measurements made at each sampling location allow for the development of longitudinal loading profiles (Fig. 3e-f) that are in turn used to identify MP sources in a quantitative manner (Table 1). This identification, based on MP load, cannot be done using concentration data alone. In the case of metal contamination from mining, the identified stream segments are further investigated to pinpoint specific inflows responsible for the mass loading (e.g., tributary inflows, small springs and/or groundwater). This follow-up activity is more complicated for MP, due to potential contributions from atmospheric transport (Wetherbee et al., 2019; Brahney et al., 2020; Sun et al., 2022), a mechanism that is not a factor in the studies of metal loading upon which this work is based (Kimball et al., 2002; Runkel et al., 2013). As such, additional techniques may be needed to further elucidate MP sources. Second, the loading analysis allows for the identification of potential removal mechanisms, such as settling from the water column to the streambed. Third, our detailed analysis of the effects of diversions would not be possible without the quantitative loading approach. As shown here, the reduction in water volume due to diversions can result in a higher relative concentration of MP at a site, and locations with seemingly high concentrations can be

erroneously considered hotspots if only concentration data are considered. Our analysis does in fact identify the site with the highest concentration as a hotspot (site B24, Section 4.3), but the associated percent contribution, loading rate (Table 1), and concentration in the absence of diversions (Fig. 3c) indicate that this stream segment is no different from the stream segments immediately upstream. This suggests that some recorded hotspots in the literature may not be the result of increased input, but rather the result of water diversions upstream of the sampling site. This finding could also have profound implications on studies of freshwater organisms, as these sudden changes in water volume could lead to higher local exposure, a factor that could be considered when assessing ecosystem health.

5. Conclusion

Our research revealed profound links between the degree of urbanization and MP concentrations, even in the investigated mountainous streams. It clearly demonstrates the worth of loading analysis for load identification per stream segments, which can lead into better source identification in the future and inform regional management and mitigation efforts. More importantly, it highlighted the crucial role of water diversions on MP concentrations and loads, with over 500 MP s^{-1} being re-distributed from the stream network into the catchment and beyond due to diversions. Clearly, these findings highlight the importance of understanding river catchments as complex systems, rather than the dendritic model through which MP only converge downstream which underlies most existing models for the simulation of global plastic fluxes from terrestrial compartments to the ocean. Our findings demonstrate that we are only beginning to uncover the true complexity of how rivers contribute to global MP flows, and that anthropogenic impacts on water management practice such as river diversions can have substantial impact on MP fate and transport.

Declaration of Competing Interest

The authors declare that they have no known competing financial interests or personal relationships that could have appeared to influence the work reported in this paper.

Data availability

Data will be made available on request.

Acknowledgments

Funding from The Leverhulme Trust via the “PlasticRivers” - The fate and transport of MPs in rivers (RPG-2017–377) project is gratefully acknowledged. S.K. was supported by the Royal Society under Fellowship INF\R2\212060 while U.S. was supported by funding from the German Research Foundation (DFG – grant number 403826296). The authors extend their gratitude towards Chantal Jackson for assistance with the graphic designs. MP samples were collected by Danja Mewes with assistance from Ron Antweiler, Mac Jones, Alex Nolan, Tanya Petach, and Ted Stets. R.R. and S.M. are supported by the U.S. Geological Survey (USGS) Ecosystem Mission Area (Climate Research & Development and Environmental Health Programs). All data supported by USGS funds are presented in Runkel et al. (2022). MP data collection and analysis were supported by non-USGS sources and are presented in this manuscript and supplement. Additional MP information may be obtained by contacting the non-USGS authors. Any use of trade, firm, or product names is for descriptive purposes only and does not imply endorsement by the U.S. Government.

Supplementary materials

Supplementary material associated with this article can be found, in the online version, at doi:10.1016/j.watres.2023.120112.

References

Anbumani, S., Kakkar, P., 2018. Ecotoxicological effects of microplastics on biota: a review. Environ. Sci. Pollut. Res. 25 (15), 14373–14396.
Barbarossa, V., Schmitt, R.J.P., Huijbregts, M.A.J., Zarfl, C., King, H., Schipper, A.M., 2020. Impacts of current and future large dams on the geographic range connectivity of freshwater fish worldwide. Proc. Natl Acad. Sci. 117 (7), 3648–3655.
Baumgartner, L.J., Marsden, T., Duffy, D., Horta, A., Ning, N., 2022. Optimizing efforts to restore aquatic ecosystem connectivity requires thinking beyond large dams. Environ. Res. Lett. 17 (1), 014008.
Bian, P., Liu, Y., Zhao, K., Hu, Y., Zhang, J., Kang, L., Shen, W., 2022. Spatial variability of microplastic pollution on surface of rivers in a mountain-plain transitional area: a case study in the Chin Ling-Wei River Plain, China. Ecotoxicol. Environ. Saf. 232, 113298.
Brahney, J., Hallerud, M., Heim, E., Hahnenberger, M., Sukumaran, S., 2020. Plastic rain in protected areas of the United States. Science 368, 1257–1260.
Campanale, C., Stock, F., Massarelli, C., Kochleus, C., Bagnuolo, G., Reifferscheid, G., Uricchio, V.F., 2020. Microplastics and their possible sources: the example of Ofanto river in southeast Italy. Environ. Pollut. 258, 113284.
Castañeda, R.A., Avlijas, S., Simard, M.A., Ricciardi, A., 2014. Microplastic pollution in St. Lawrence River sediments. Can. J. Fish. Aquat.Sci. 71 (12), 1767–1771.
Coffin, S., 2023. The emergence of microplastics: charting the path from research to regulations. Environ. Sci. 2 (3), 356–367.
Dalmau-Soler, J., Ballesteros-Cano, R., Boleda, M.R., Paraira, M., Ferrer, N., Lacorte, S., 2021. Microplastics from headwaters to tap water: occurrence and removal in a drinking water treatment plant in Barcelona Metropolitan area (Catalonia, NE Spain). Environ. Sci. Pollut. Res. 28 (42), 59462–59472.
de Carvalho, A.R., Garcia, F., Riem-Galliano, L., Tudesque, L., Albignac, M., ter Halle, A., Cucherousset, J., 2021. Urbanization and hydrological conditions drive the spatial and temporal variability of microplastic pollution in the Garonne River. Sci. Total Environ. 769, 144479.
Drummond, J.D., Nel, H.A., Packman, A.I., Krause, S., 2020. Significance of hyporheic exchange for predicting microplastic fate in rivers. Environ. Sci. Technol. Lett. 7 (10), 727–732.
Drummond, J.D., Schneidewind, U., Li, A., Hoellein, T.J., Krause, S., Packman, A.I., 2022. Microplastic accumulation in riverbed sediment via hyporheic exchange from headwaters to mainstems. Sci. Adv. 8 (2), eabi9305.
Edwards, T.K., aand Glysson, G.D., 1999. Field methods for measurement of fluvial sediment, U.S. Geological Survey, Techniques of Water-Resources Investigations, Book 3, Chapter C2, Reston, Virginia.
ESRI, 2011. ArcGIS Desktop: Release 10. Environmental Systems Research Institute, Redlands, CA.
Ferraz, M., Bauer, A.L., Valiati, V.H., Schulz, U.H., 2020. Microplastic concentrations in raw and drinking water in the Sinos river, Southern Brazil. Water 12 (11), 3115.
Frenken, K.a.G., V. 2012 Irrigation water requirement and water withdrawal by country. Nations, F.-T.F.a.A.O.o.t.U. (ed).
Grbić, J., Helm, P., Athey, S., Rochman, C.M., 2020. Microplastics entering northwestern Lake Ontario are diverse and linked to urban sources. Water Res. 174, 115623.
Hartmann, N.B., Hüffer, T., Thompson, R.C., Hassellöv, M., Verschoor, A., Daugaard, A. E., Rist, S., Karlsson, T., Brennholt, N., Cole, M., Herrling, M.P., Hess, M.C., Ivleva, N. P., Lusher, A.L., Wagner, M., 2019. Are we speaking the same language? recommendations for a definition and categorization framework for plastic debris. Environ. Sci. Technol. 53 (3), 1039–1047.
Hurley, R., Woodward, J., Rothwell, J.J., 2018. Microplastic contamination of river beds significantly reduced by catchment-wide flooding. Nat. Geosci. 11 (4), 251–257.
Jiang, C., Yin, L., Li, Z., Wen, X., Luo, X., Hu, S., Yang, H., Long, Y., Deng, B., Huang, L., Liu, Y., 2019. Microplastic pollution in the rivers of the Tibet Plateau. Environ. Pollut. 249, 91–98.
Jin, X., Fu, X., Lu, W., Wang, H., 2022. Fugitive release and influencing factors of microplastics in urbanized watersheds: a case study of the central area of Suzhou City. Sci. Total Environ. 837, 155653.
Kelleher, L., Schneidewind, U., Krause, S., Haverson, L., Allen, S., Allen, D., Kukkola, A., Murray-Hudson, M., Maselli, V., Franchi, F., 2023. Microplastic accumulation in endorheic river basins—the example of the Okavango Panhandle (Botswana). Sci. Total Environ. 874, 162452.
Kimball, B.A., Runkel, R.L., Walton-Day, K., Bencala, K.E., 2002. Assessment of metal loads in watersheds affected by acid mine drainage by using tracer injection and synoptic sampling: cement Creek, Colorado, USA. Appl. Geochem. 17 (9), 1183–1207.
Krause, S., Baranov, V., Nel, H.A., Drummond, J.D., Kukkola, A., Hoellein, T., Sambrook Smith, G.H., Lewandowski, J., Bonet, B., Packman, A.I., Sadler, J., Inshyna, V., Allen, S., Allen, D., Simon, L., Mermillod-Blondin, F., Lynch, .I.., 2021. Gathering at the top? Environmental controls of microplastic uptake and biomagnification in freshwater food webs. Environ. Pollut. 268, 115750.
Kukkola, A., Krause, S., Lynch, I., Sambrook Smith, G.H., Nel, H., 2021. Nano and microplastic interactions with freshwater biota—current knowledge, challenges and future solutions. Environ. Int. 152, 106504.
Kukkola, A., Krause, S., Yonan, Y., Kelleher, L., Schneidewind, U., Sambrook Smith, G.H., Nel, H., Lynch, I., 2023. Easy and accessible way to calibrate fluorescence

microscope and to create a microplastic identification key. MethodsX 10, 102053. https://doi.org/10.1016/j.mex.2023.102053.
Kukkola, A.T., Senior, G., Maes, T., Silburn, B., Bakir, A., Kröger, S., Mayes, A.G., 2022. A large-scale study of microplastic abundance in sediment cores from the UK continental shelf and slope. Mar. Pollut. Bull. 178, 113554.
Kumar, R., Sharma, P., Manna, C., Jain, M., 2021. Abundance, interaction, ingestion, ecological concerns, and mitigation policies of microplastic pollution in riverine ecosystem: a review. Sci. Total Environ. 782, 146695.
Kurki-Fox, J.J., Doll, B.A., Monteleone, B., West, K., Putnam, G., Kelleher, L., Krause, S., Schneidewind, U., 2023. Microplastic distribution and characteristics across a large river basin: insights from the Neuse River in North Carolina, USA. Sci. Total Environ. 878, 162940.
Lambert, S., Wagner, M., 2018. Microplastics Are Contaminants of Emerging Concern in Freshwater Environments: An Overview. In: Wagner, M., Lambert, S. (Eds.), Freshwater Microplastics, The Handbook of Environmental Chemistry, Vol 58. Springer International Publishing, Cham, pp. 1–23.
Lebreton, L., Egger, M., Slat, B., 2019. A global mass budget for positively buoyant macroplastic debris in the ocean. Sci. Rep. 9 (1), 12922.
Lebreton, L.C.M., van der Zwet, J., Damsteeg, J.-.W., Slat, B., Andrady, A., Reisser, J., 2017. River plastic emissions to the world's oceans. Nat. Commun. 8 (1), 15611.
Lenz, R., Enders, K., Stedmon, C.A., Mackenzie, D.M.A., Nielsen, T.G., 2015. A critical assessment of visual identification of marine microplastic using Raman spectroscopy for analysis improvement. Mar. Pollut. Bull. 100 (1), 82–91.
Leslie, H.A., Brandsma, S.H., van Velzen, M.J.M., Vethaak, A.D., 2017. Microplastics en route: field measurements in the Dutch river delta and Amsterdam canals, wastewater treatment plants, North Sea sediments and biota. Environ. Int. 101, 133–142.
Margenat, H., Nel, H.A., Stonedahl, S.H., Krause, S., Sabater, F., Drummond, J.D., 2021. Hydrologic controls on the accumulation of different sized microplastics in the streambed sediments downstream of a wastewater treatment plant (Catalonia, Spain). Environ. Res. Lett. 16 (11), 115012.
McGivney, E., Cederholm, L., Barth, A., Hakkarainen, M., Hamacher-Barth, E., Ogonowski, M., Gorokhova, E., 2020. Rapid physicochemical changes in microplastic induced by biofilm formation. Front. Bioeng. Biotechnol. 8.
Meijer, L.J., van Emmerik, T., van der Ent, R., Schmidt, C., Lebreton, L., 2021. More than 1000 rivers account for 80% of global riverine plastic emissions into the ocean. Sci. Adv. 7 (18), eaaz5803.
Murphy, S.F., 2006. State of the watershed: water quality of boulder creek, 1284. U.S. Geological Survey Circular, Colorado, p. 34. https://doi.org/10.3133/cir1284.
Nel, H.A., Sambrook Smith, G.H., Harmer, R., Sykes, R., Schneidewind, U., Lynch, I., Krause, S., 2020. Citizen science reveals microplastic hotspots within tidal estuaries and the remote Scilly Islands, United Kingdom. Mar. Pollut. Bull. 161, 111776.
Ockelford, A., Cundy, A., Ebdon, J.E., 2020. Storm response of fluvial sedimentary microplastics. Sci. Rep. 10 (1), 1865.
OECD 2022. The Organisation for Economic Co-operation and Development. Freshwater abstractions (million m3). Retrieved from: https://stats.oecd.org/Index.aspx?DataSetCode=WATER_ABSTRACT.
R Core Team (2022). R: a language and environment for statisticalcomputing. R Foundation for Statistical Computing, Vienna, Austria.*URL https://www.R-project.org/*.
Reynolds, R.L., Goldstein, H.L., Kokaly, R.F. and Derry, J. 2022 Microplastic particles in dust-on-snow, Upper Colorado River Basin, Colorado Rocky Mountains, 2013–16, Reston, VA.
Runkel, R.L., Murphy, S.F., Stets, E., Nolan, A.J., Roth, D.A., Repert, D.A., and Qi, S.L., 2022, Diel and synoptic sampling data from Boulder Creek and South Boulder Creek, near Boulder, Colorado, September-October 2019: U.S. Geological Survey data release, 10.5066/P95Q26YR.
Runkel, R.L., Walton-Day, K., Kimball, B.A., Verplanck, P.L., Nimick, D.A., 2013. Estimating instream constituent loads using replicate synoptic sampling, Peru Creek, Colorado. J. Hydrol. 489, 26–41.
Samandra, S., Johnston, J.M., Jaeger, J.E., Symons, B., Xie, S., Currell, M., Ellis, A.V., Clarke, B.O., 2022. Microplastic contamination of an unconfined groundwater aquifer in Victoria, Australia. Sci. Total Environ. 802, 149727.
Schmidt, C., Krauth, T., Wagner, S., 2017. Export of Plastic Debris by Rivers into the Sea. Environ. Sci. Technol. 51 (21), 12246–12253.
Shen, M., Song, B., Zhu, Y., Zeng, G., Zhang, Y., Yang, Y., Wen, X., Chen, M., Yi, H., 2020. Removal of microplastics via drinking water treatment: current knowledge and future directions. Chemosphere 251, 126612.
Siegfried, M., Koelmans, A.A., Besseling, E., Kroeze, C., 2017. Export of microplastics from land to sea. A modelling approach. Water Res. 127, 249–257.
Sun, J., Peng, Z., Zhu, Z.-.R., Fu, W., Dai, X., Ni, B.-.J., 2022. The atmospheric microplastics deposition contributes to microplastic pollution in urban waters. Water Res. 225, 119116.
Talbot, R., Chang, H., 2022. Microplastics in freshwater: a global review of factors affecting spatial and temporal variations. Environ. Pollut. 292, 118393.
Tibbetts, J., Krause, S., Lynch, I., Sambrook Smith, G.H., 2018. Abundance, distribution, and drivers of microplastic contamination in urban river environments. Water (Basel) 10 (11), 1597.
U.S. Geological Survey, 2019, The StreamStats program, online at https://streamstats.usgs.gov/ss/, accessed January 2023.
Uzun, P., Farazande, S., Guven, B., 2022. Mathematical modeling of microplastic abundance, distribution, and transport in water environments: a review. Chemosphere 288 (2), 132517. Pt.
van Wijnen, J., Ragas, A.M.J., Kroeze, C., 2019. Modelling global river export of microplastics to the marine environment: sources and future trends. Sci. Total Environ. 673, 392–401.
Wagner, S., Klöckner, P., Stier, B., Römer, M., Seiwert, B., Reemtsma, T., Schmidt, C., 2019. Relationship between discharge and river plastic concentrations in a rural and an urban catchment. Environ. Sci. Technol. 53 (17), 10082–10091.
Wang, T., Wang, J., Lei, Q., Zhao, Y., Wang, L., Wang, X., Zhang, W., 2021. Microplastic pollution in sophisticated urban river systems: combined influence of land-use types and physicochemical characteristics. Environ. Pollut. 287, 117604.
Wetherbee, G.A., Baldwin, A.K. and Ranville, J.F. 2019 It is raining plastic, U.S. Geological Survey Open-File Report 2019–1048, Reston, VA. 10.3133/ofr20191048.
Wetherbee, G.A., Murphy, S.F., Repert, D.A., Heindel, R.C., and Liethen, E.A. 2021 Chemical analyses and precipitation depth data for wet deposition samples collected as part of the National Atmospheric Deposition Program in the Colorado Front Range, 2017-2019. release, U.S.G.S.d. (ed).
Wong, G., Löwemark, L., Kunz, A., 2020. Microplastic pollution of the Tamsui River and its tributaries in northern Taiwan: spatial heterogeneity and correlation with precipitation. Environ. Pollut. 260, 113935.
Wu, P., Tang, Y., Dang, M., Wang, S., Jin, H., Liu, Y., Jing, H., Zheng, C., Yi, S., Cai, Z., 2020. Spatial-temporal distribution of microplastics in surface water and sediments of Maozhou River within Guangdong-Hong Kong-Macao Greater Bay Area. Sci. Total Environ. 717, 135187.
Yuan, W., Christie-Oleza, J.A., Xu, E.G., Li, J., Zhang, H., Wang, W., Lin, L., Zhang, W., Yang, Y., 2022. Environmental fate of microplastics in the world's third-largest river: basin-wide investigation and microplastic community analysis. Water Res. 210, 118002.
Zhang, Y., Gao, T., Kang, S., Allen, S., Luo, X., Allen, D., 2021. Microplastics in glaciers of the Tibetan Plateau: evidence for the long-range transport of microplastics. Sci. Total Environ. 758, 143634.